

## Domain Decomposition methods on nonmatching grids and some applications to linear elasticity problems

*Domain decomposition techniques provide a powerful tool for the coupling of different discretization methods or nonmatching triangulations across subregion boundaries. Here, we consider mortar finite elements methods for linear elasticity and diffusion problems. These domain decomposition techniques provide a more flexible approach than standard conforming formulations. The mortar solution is weakly continuous at subregion boundaries, and its jump is orthogonal to a suitable Lagrange multiplier space. Our approach is based on dual bases for the Lagrange multiplier space. It has the advantage of locally supported basis functions for the constrained space. This is not true for the standard mortar method [2]. The biorthogonality relation guarantees that the Lagrange multiplier can be locally eliminated, and that we obtain a symmetric positive semidefinite system on the unconstrained product space. This system will be solved by multigrid techniques. Numerical results illustrate the performance of the multigrid method in 2D and 3D.*

### 1. Introduction

The central idea of domain decomposition techniques is to decompose a global problem into subproblems of smaller complexity, and to “glue” the subproblems together in a suitable way. This is especially helpful for problems given on complicated geometries or problems with jumps in the material coefficients. Numerical examples for these situations will be given in the last section. As model problem let us consider the following linear elasticity problem with homogeneous Dirichlet boundary conditions

$$\sum_{j=1}^d \frac{\partial}{\partial x_j} \left( \sum_{l,m=1}^d E_{ijlm} \frac{\partial u_l}{\partial x_m} \right) = f_i \quad \text{in } \Omega.$$

Here,  $\Omega$  is a bounded, polygonal domain in  $\mathbb{R}^d$ ,  $d = 2, 3$  and Hooke’s tensor  $E$  is assumed to be sufficiently smooth and uniformly positive definite. The components of  $f \in (L^2(\Omega))^d$  are denoted by  $f_i$ ,  $1 \leq i \leq d$ .

We use a geometrically conforming decomposition of  $\Omega$  into  $K$  non-overlapping polyhedral subdomains  $\Omega_k$ , i.e.,  $\bar{\Omega} = \cup_{k=1}^K \bar{\Omega}_k$ . Each subdomain is associated with an independent triangulations. Let us remark that the triangulations do not have to match at the common interface between two adjacent subdomains. The interfaces are denoted by  $\gamma_m$ ,  $1 \leq m \leq M$ , and inherit their triangulation from one of the adjacent subdomains. This side is called non-mortar side and the opposite one mortar side. The choice is arbitrary but fixed. We use standard piecewise linear in 2D and piecewise trilinear in 3D conforming finite elements on the subdomains and denote the product space by  $X_h$ . Then, the constrained mortar space  $V_h$  is defined by:  $V_h := \{v \in X_h \mid b(v, \mu) = 0, \mu \in M_h\}$ , where the bilinear form  $b(\cdot, \cdot)$  is given as a duality pairing on the interfaces  $b(v, \mu) := \sum_{m=1}^M \langle [v], \mu \rangle_{\gamma_m}$ ,  $v \in X_h$ ,  $\mu \in M_h$ , and  $[v]$  is the jump of  $v$  on  $\gamma_m$ . The constrained space  $V_h$  consist of all functions in  $X_h$  which have a vanishing jump at the interface with respect to the Lagrange multiplier space  $M_h$ . Of crucial importance is the suitable choice of  $M_h := \prod_{m=1}^M (M_h(\gamma_m))^d$  in the definition of the constrained space  $V_h$ . The space  $M_h(\gamma_m)$  is defined by  $\nu_m$  locally supported linear independent functions  $\psi_l^m$ . Here,  $\nu_m := \dim W_{0;h}(\gamma_m)$ , and  $W_h(\gamma_m)$  is the finite element trace space on  $\gamma_m$  and  $W_{0;h}(\gamma_m) := W_h(\gamma_m) \cap H_0^1(\gamma_m)$ . Now, the nonconforming mortar solution is obtained by: Find  $u_h \in V_h$  such that

$$a(u_h, v) = (f, v)_0, \quad v \in V_h. \tag{1}$$

Here, the bilinear form  $a(\cdot, \cdot)$  is given as  $a(u, v) := \sum_{k=1}^K \sum_{i,j,l,m=1}^d \int_{\Omega_k} E_{ijlm} \frac{\partial u_l}{\partial x_m} \frac{\partial v_i}{\partial x_j} dx$ ,  $u, v \in X_h$ . If  $P_0(\gamma_m) \subset M_h(\gamma_m)$ , the bilinear form  $a(\cdot, \cdot)$  is uniformly elliptic on  $V_h \times V_h$ . Under some assumption on  $M_h(\gamma_m)$ , optimal a priori bounds for the discretization error for the mortar finite element solution are obtained in the energy norm and the  $L^2$ -norm, we refer to [2,5,7].

**Dual bases for the Lagrange multiplier space.** Here, we consider two different types of dual bases in 2D and 3D. The first one is spanned by piecewise linear functions and the second one by piecewise constants. Figure 1 illustrates the shape of the dual basis functions. In the left part, the 2D case is depicted whereas in the right part, the isolines of a dual basis function at the two dimensional interface in 3D are given. In 2D, the support of our dual

basis functions is the union of exactly two adjacent edges, and in 3D it is in the interior of  $\gamma_m$  the union of four faces sharing one vertex. We remark that the definition of the basis functions associated with the vertex  $x_k^m$  has to be modified if  $x_k^m$  is close to the boundary of  $\gamma_m$ , for details we refer the reader to [2,7]. In both cases, it is easy to

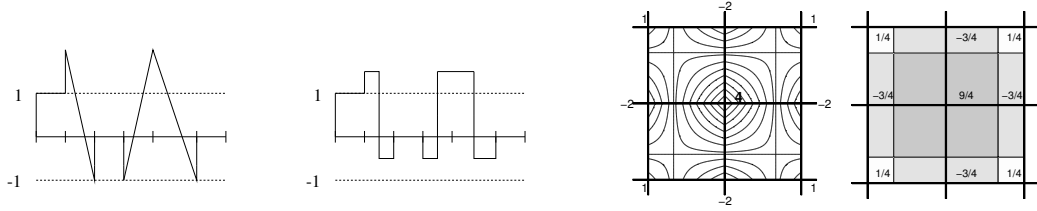


Figure 1: Piecewise constant and piecewise linear dual basis functions in 2D (left) and 3D (right)

see that the biorthogonality relation  $\int_{\gamma_m} \phi_l^m \psi_k^m d\sigma = \delta_{lk} \int_{\gamma_m} \phi_l^m d\sigma$  holds, where  $\phi_l^m$  and  $\psi_k^m$  denote the nodal basis functions of  $W_{0;h}(\gamma_m)$  and  $M_h(\gamma_m)$ , respectively. We refer to [7], for an analysis of the discretization error and some numerical results illustrating the influence of different Lagrange multiplier spaces. Of crucial importance is the so called mortar projection which is  $H_{00}^{1/2}$ -stable. Optimal a priori estimates in the energy norm and the  $L^2$ -norm can be obtained.

## 2. Multigrid method on the product space

Let us assume that we have a nested sequence of global triangulations and let us denote the associated unconstrained product spaces by  $X_l$ ,  $0 \leq l \leq L$ . The meshsize is given by  $h_l = 2h_{l+1}$ . In contrast to the constrained spaces  $V_l$ , the product spaces  $X_l$  are nested. We denote the standard prolongation operator by  $I_{l-1}^l : X_{l-1} \rightarrow X_l$  and the restriction by  $I_l^{l-1} : X_l \rightarrow X_{l-1}$ . Here, we use a symmetric positive semidefinite variational problem on the unconstrained product space  $X_l$  which is given in terms of a projection  $P_l$ . We start with the definition of the locally defined projection operator  $P_l : X_l \rightarrow X_l$

$$(P_l v)_i := \sum_{m=1}^M \sum_{l=1}^{\nu_m} \alpha_{m,l}^i \frac{b(v_i, \psi_l^m)}{\int_{\gamma_m} \phi_l^m d\sigma} \phi_l^m, \quad 1 \leq i \leq d,$$

where the nodal basis functions  $\phi_l^m$  of  $W_{0;l}(\gamma_m)$  are extended in a trivial way on the non-mortar side of  $\gamma_m$ . Then, it is easy to see that the kernel of  $P_l$  is exactly the constrained space  $V_l$ . Let  $A_l$ ,  $B_l$ , and  $C_l$  be the matrices associated with the bilinear forms  $a(\cdot, \cdot)$  on  $X_l \times X_l$ ,  $b(\cdot, \cdot)$  on  $X_l \times M_l$  and the projection  $P_l$ , respectively, and  $f_l$  the vector associated with the right hand side.

Lemma 1. *The following system is symmetric and positive definite. Its solution  $u_l \in X_l$  satisfies  $u_l \in V_l$  and (1)*

$$\hat{A}_l v_l := ((\text{Id} - C_l^T)A_l(\text{Id} - C_l) + C_l^T A_l C_l) u_l = (\text{Id} - C_l^T) f_l. \quad (2)$$

Furthermore, the solution  $u_l$  can be obtained by  $u_l = (\text{Id} - C_l) v_l$  from any solution  $v_l \in X_l$  of

$$\tilde{A}_l u_l := (\text{Id} - C_l^T) A_l (\text{Id} - C_l) v_l = (\text{Id} - C_l^T) f_l. \quad (3)$$

Proof. It is easy to see that  $\hat{A}_l$  and  $\tilde{A}_l$  are symmetric and positive semidefinite. Furthermore,  $A_l$  is positive definite on  $V_l$  and  $P_l X_l$ . Then, the triangle inequality yields that  $\hat{A}_l$  is positive definite. Now, let  $u_l \in V_l$  be the solution of (1), i.e.,  $(\text{Id} - C_l^T) A_l u_l = (\text{Id} - C_l^T) f_l$ , then by definition of  $C_l$  we find  $C_l u_l = 0$  and  $u_l$  solves (2). Observing that  $C_l$  is a projection, the second assertion follows immediately.

In the following, we call  $v_l \in X_l$  a solution of (3) only if it satisfies (3) and if  $v_l \in V_l$ . To obtain level independent convergence rates for our multigrid method, suitable approximation and smoothing properties have to be established. In a first step, we consider level dependent grid transfer operators  $(I_{\text{mod}})_l^{l-1}$  and  $(I_{\text{mod}})_{l-1}^l$  defined by

$$(I_{\text{mod}})_l^{l-1} := (\text{Id} - C_{l-1}^T) I_l^{l-1}, \quad (I_{\text{mod}})_{l-1}^l := (\text{Id} - C_l) I_{l-1}^l.$$

It is easy to see that these transfer operators guarantee  $C_{l-1}^T (I_{\text{mod}})_l^{l-1} w_l = 0$ ,  $w_l \in X_l$ , and  $C_l (I_{\text{mod}})_{l-1}^l w_{l-1} = 0$ ,  $w_{l-1} \in X_{l-1}$ . Then, an appropriate approximation property can be found in [9]. It is based on the assumption that the iterate after the smoothing steps is in the constrained space  $V_l$ . Starting with an arbitrary smoother for  $\tilde{A}_l$ , we construct a modified one satisfying this condition. Let  $G_l^{-1}$  be a smoother for  $\tilde{A}_l$ , e.g., a damped Jacobi method. Then, we define our modified smoother by  $\tilde{G}_l^{-1} := (\text{Id} - C_l) G_l^{-1} (\text{Id} - C_l^T)$ , and denote the iterates by  $y_l^i$  and  $\tilde{y}_l^i$ , respectively. The following lemma shows the relation between the two different iterates.

Lemma 2. Under the assumption  $\tilde{y}_l^0 = (\text{Id} - C_l)y_l^0$ , the iterates  $\tilde{y}_l^i$  can be obtained from  $y_l^i$  by a local post-processing step

$$\tilde{y}_l^i = (\text{Id} - C_l)y_l^i, \quad i \geq 1.$$

Furthermore, the smoothing and stability properties of  $\tilde{G}_l^{-1}$  are inherited from  $G_l^{-1}$ , i.e.,

$$\|\tilde{A}_l \tilde{e}_l^i\| = \|\tilde{A}_l e_l^i\|, \quad \|\tilde{e}_l^i\| \leq C \|e_l^i\|,$$

where  $\tilde{e}_l^i$  and  $e_l^i$  are the corresponding iteration errors and the constant  $C < \infty$  does not depend on the level  $l$ .

Proof. Observing the special structure of the right hand side  $d_l$  and  $\tilde{A}_l$ , we obtain by induction

$$\tilde{y}_l^{i+1} = \tilde{y}_l^i + (\text{Id} - C_l)G_l^{-1}(\text{Id} - C_l^T)(d_l - \tilde{A}_l \tilde{y}_l^i) = (\text{Id} - C_l)(y_l^i + G_l^{-1}(d_l - \tilde{A}_l y_l^i)) = (\text{Id} - C_l)y_l^{i+1}.$$

The second assertion follows from the observation that  $C_l$  is a scaled mass matrix, the norm of which is bounded independently of  $l$ .

Our multigrid method for the solution of (1) will be defined in terms of the equation (3), the given modified transfer operators, the smoother  $\tilde{G}_l^{-1}$ , the implementation of which is realized in terms of  $G_l^{-1}$  and one local post-processing steps at the end of the smoothing iterations. Then, we obtain level independent convergence rates for the  $\mathcal{W}$ -cycle provided that the number of smoothing steps is large enough.

### 3. Numerical results

Here, we consider some numerical results illustrating the performance of our multigrid method in 2D and 3D. Our multigrid method has been implemented for scalar problems and systems of equations for 2D and 3D in the finite element toolbox UG, see [1]. We apply nested iteration and use a tolerance of  $5 \cdot 10^{-8}$  for the norm of the residuum as stopping criterion for the iteration. Our first example is a 2D plane strain example with discontinuous coefficients, discretized by linear finite elements on triangles. The computational domain is depicted in the left picture in Figure 2, and consists of a nut and a wrench. Dirichlet boundary conditions are applied at the handle of the wrench, i.e.,  $u_1(x, y) = 1/3 \cdot \|m - (x, y)^T\| \cdot \sin(\alpha)$ ,  $u_2(x, y) = 1/3 \cdot \|m - (x, y)^T\| \cdot (1 - \cos(\alpha))$ , and homogenous Dirichlet conditions at the interior boundary of the nut. Here,  $m$  denotes the midpoint of the nut and we set  $\alpha = \pi/30$ . The interface is located at the contact area between the nut and the wrench. We use a  $\mathcal{W}(3, 3)$ -cycle with a symmetric Gauß-Seidel smoother accelerated by a stabilized biconjugate gradient method (bicgstab). Table 1 shows the required number of iterations on each level and the number of unknowns. As it can be seen, the number of iterations is independent of the level. The distorted grid scaled by a factor of 10 is shown in the second picture from the left in Figure 2. An adaptive refinement strategy has been used, controlled by a residual based error estimator for mortar finite elements.

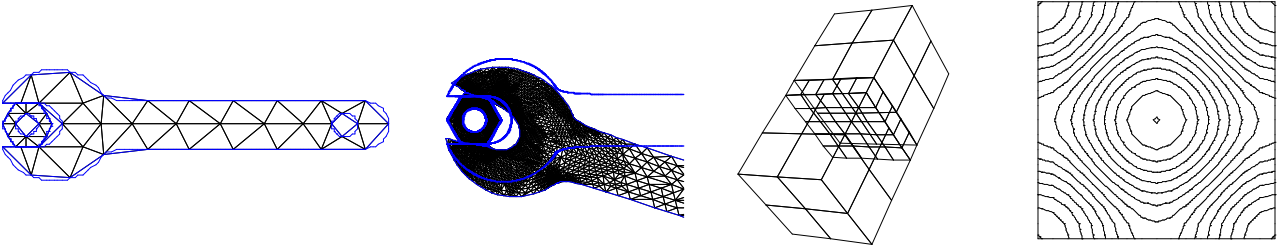


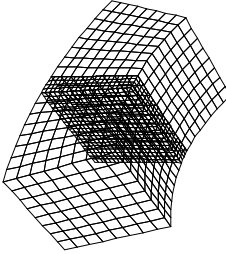
Figure 2: Initial and final triangulation in 2D (left) and initial triangulation and isolines in 3D (right)

As 3D example, we consider a "Sandwich"-like domain build up of two different materials. The domain  $\Omega$  is decomposed into three hexahedrons  $\bar{\Omega}_i := \{[0, 1]^2 \times [z_i, z_{i+1}]\}$  where  $z_1 := 0, z_2 := 1, z_3 := 1.2, z_4 := 2.2$ . In the right part of Figure 2, the nonmatching initial triangulation is shown. The non-mortar sides are defined on the middle hexahedron. We consider two different elliptic problems on this domain: a scalar model problem and a full linear elasticity problem, both with discontinuous coefficients. For both problems, we use the same initial triangulation, see Figure 2. We refer to the right picture in Figure 2 for the isolines of the solution at the interface in the scalar case.

Let us first consider the scalar problem  $-\text{div } a \nabla u = 1$ , on  $\Omega := (0, 1)^2 \times (0, 2.2)$  where the coefficient  $a$  is piecewise constant,  $a|_{\Omega_i} := 100, i = 1, 3$  and  $a|_{\Omega_2} := 1$ . Dirichlet boundary conditions are applied on the upper and lower part of the domain,  $u(x, y, z) = 1000 \sqrt{(x - 1/2)^2 + (y - 1/2)^2} \cdot (1.0 - y/3) \exp(-10(x^2 + y^2))$  if  $z = z_1$  or  $z = z_4$ , and homogeneous Neumann boundary conditions are taken on the remaining part of the boundary. In Figure 3, the

asymptotic convergence rates for the Jacobi and the Gauß–Seidel smoother are depicted. The numerical results show that the asymptotic convergence rates do not depend on the refinement level. Even for the  $\mathcal{V}(1, 1)$ –cycle, a constant asymptotic convergence rate is obtained. For the full linear elasticity example, we took as material parameters for

Level	# dof	# iter
0	108	1
1	232	3
2	904	4
3	1,622	4
4	2,350	4
5	3,478	5
6	5,380	5
7	8,272	5
8	12,844	5
9	20,130	5
10	30,878	5



Level	# dof	# iter
0	378	1
1	1,839	2
2	10,989	2
3	74,865	2
4	550,233	2

Table 1: Numerical results for the 2D example (left), the distorted grid (middle) and the 3D results (right)

the Lamé constants  $\mu|_{\Omega_i} = 8517$  and  $\lambda|_{\Omega_i} = 108280$  for  $i = 1, 3$  and  $\mu|_{\Omega_i} = 2008$  and  $\lambda|_{\Omega_i} = 3567$  for  $i = 2$ . Here, we apply an incomplete  $LU$ –decomposition as smoother and use the  $\mathcal{V}(3, 3)$ –cycle as preconditioner for the bcgstab–method. Dirichlet conditions are applied on the top and bottom of the ”Sandwich”, Neumann boundary conditions on the remaining part of the boundary. The right table in Table 1 shows the performance of our method in 3D. Although the number of unknowns increases by a factor of 10 in every refinement step, the number of iterations to achieve the required tolerance is constant. We remark, that uniform refinement has been used for this example. The displacement of the solution scaled by a factor of 10 is shown in the middle of Table 1.

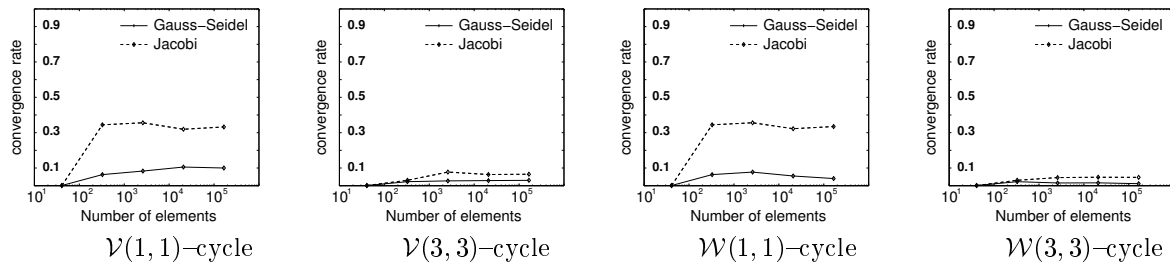


Figure 3: Asymptotic conv. rates for Jacobi and symmetric Gauß–Seidel smoother (3D scalar example)

#### 4. References

- 1 BASTIAN, P.; BIRKEN, K.; JOHANNSEN, K.; LANG, S.; NEUSS, N.; RENTZ–REICHERT, H.; AND WIENERS, C.: UG – a flexible software toolbox for solving partial differential equations. *Computing and Visualization in Science* 1 (1997), 27–40.
- 2 BERNARDI, C.; MADAY, Y.; AND PATERA, A.: Domain decomposition by the mortar element method, In H. Kaper et al., editors *Asymptotic and numerical methods for partial differential equations with critical parameters*. pages 269–286, 1993, Reidel, Dordrecht.
- 3 GOPALAKRISHNAN, G; AND PASCIAK, J.: Multigrid for the mortar finite element method. *to appear in SIAM J. Numer. Anal.*, 2000.
- 4 HACKBUSCH, W.: *Multi-Grid Methods and Applications*. Springer, 1985.
- 5 WOHLMUTH, B.: A mortar finite element method using dual spaces for the Lagrange multiplier. *to appear in SIAM J. Numer. Anal.*, 2000.
- 6 WOHLMUTH, B.; AND KRAUSE, R.: Multigrid methods based on the unconstrained product space arising from mortar finite element discretizations. *Preprint FUB A-18*, 1999.
- 7 WOHLMUTH, B.: Discretization Methods and Iterative Solvers Based on Domain Decomposition. *Habilitationschrift*, Universität Augsburg, 1999.

Addresses: ROLF H. KRAUSE, Inst. für Mathematik, FU Berlin, 14 195 Berlin, Germany,  
email: krause@math.fu-berlin.de

BARBARA I. WOHLMUTH, Math. Institut, Universität Augsburg, 86 159 Augsburg, Germany,  
email: wohlmuth@math.uni-augsburg.de